Proceedings of the 7th International Conference on HydroScience and Engineering

Philadelphia, USA September 10-13, 2006 (ICHE 2006)

ISBN: 0977447405

Drexel University

College of Engineering

FLUID FLOW CONDITIONS IN ASYMMETRICAL NOZZLE IN DISCHARGE PIPE SYSTEM OF REVERSIBLE PUMP-TURBINE

Andrej PREDIN[1], Roman KLASINC[2], Ignacijo BILUŠ[3], Mitja KASTREVC[4]

ABSTRACT

Modern reversible hydro energetic systems are expected to have short switching time during operating regime (pump-turbine). It is known, on the one hand, that profit of reversible systems increases with difference between the buying and selling price of the produced electrical energy. When the switching time is reducing, on the other hand, the physical limitations appeared. The water hammer effect and pressure pulsations have to be considered, because of flow inertia. These limitations could lead to material erosion and damage. This paper presents an asymmetrical nozzle that is a simple but effective approach to avoid water hammer effects in pipe systems. Nozzle in the pipe is used to reduce the water hammer effect, during sudden stop of the system, regardless the system is operating in turbine or pump mode. Special attention should be given to the design of the nozzle, due to recirculation flows that can be induced with inappropriate geometry. Accordingly, computational fluid dynamics was used for nozzle design and to analyze the flow at different operating conditions. Numerical simulation results were compared to experimental measurements from a physical model of a reversible pump-turbine. The results for the pressure and overall characteristics of the flow match enough, that could be conclude that the correct flow pattern is captured in both operating regimes.

1. INTRODUCTION

Presented nozzle flow investigations are part of the larger project KOPS II, which is a power plant in the western part of Austria. The power plant performs as reversible pump storage, with a head H=800 m, capacity Q=26.7 m^3/s, and three 150 MW vertical 6 nozzle Pelton turbines. The analyzed nozzle is located in the pipe between the upper and lower surge tank as shown in Figure 1, and it is used to damp flow pulsations and reduce the water hammer effect (Bergant 2003) when the system (turbine or pump regime) is suddenly stop. The lower chamber or surge tank is treated as a discharging pipe system of the turbine/pump.

[1] Associate Professor Dr., Faculty of Mechanical engineering, University of Maribor, Smetanova 17, SI-2000 Maribor, SLOVENIA. (Andrej.Predin@uni-mb.si)

[2] Associate Professor Dr., Institute for Hydraulic Resources and Water Management, Graz Technology University, Stremayer gasse 11/B A-0000 Graz AUSTRIA (Roman.Klasinc@tugraz.at)

[3] Assistant Dr., Faculty of Mechanical engineering, University of Maribor, Smetanova 17, SI-2000 Maribor, SLOVENIA. (Ignacijo.Bilus@uni-mb.si)

[4] Researcher Dr., Faculty of Mechanical engineering, University of Maribor, Smetanova 17, SI-2000 Maribor, SLOVENIA. (Mitja.Kastrevc@uni-mb.si)

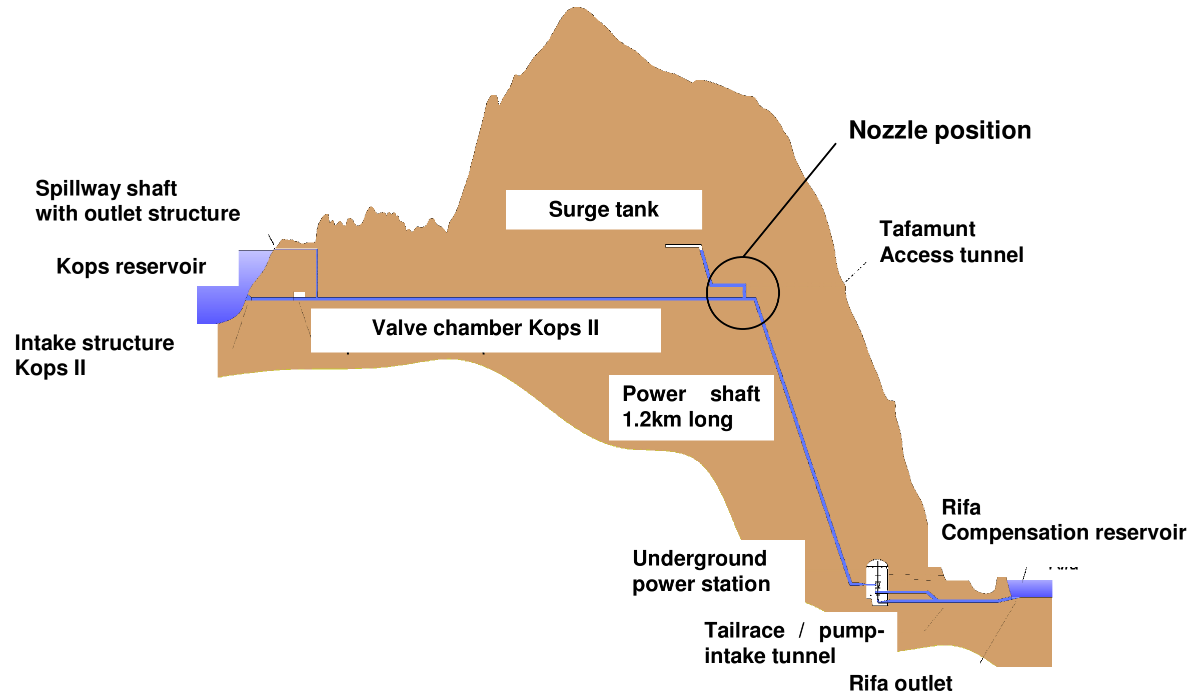

Figure 1 Project KOPS II layout showing nozzle position in the piping system.

2. EXPERIMENTAL ANALYZE

a) 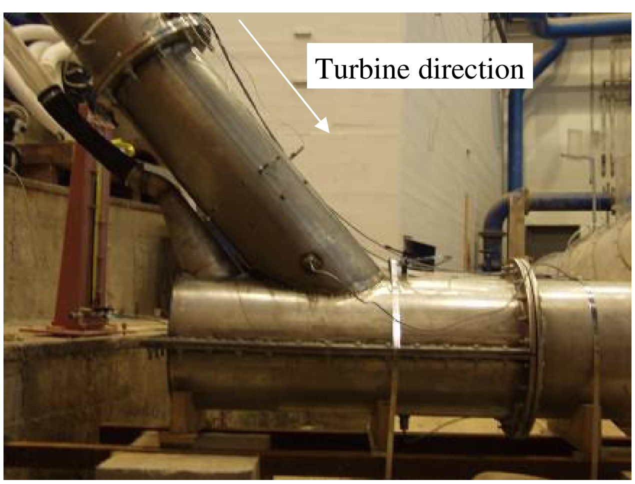

b) 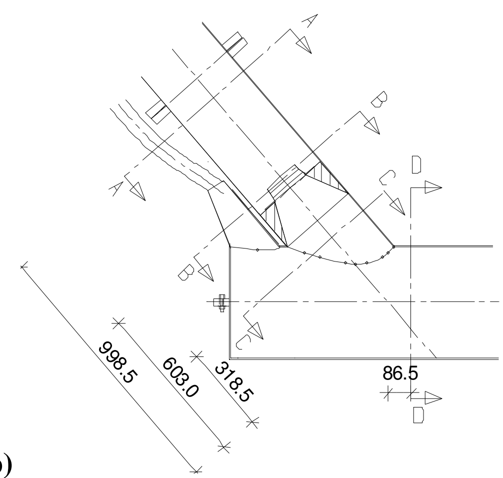

Figure 2 Nozzle in the experimental test ring (a), and (b) position of pressure transducers.

The measurements are taken on a physical model built in the scale of 1:17. The nozzle is located in the pipe system that connecting the surge tanks. Four measurement planes are located in the vicinity of the nozzle, shown as sections A-A, B-B, C-C, and D-D in Figure 2(b). At each section, six pressure transducers are placed in the pipe wall, evenly spaced around the pipe circumference. The

PHILIPS relative pressure transducers were used with accuracy up to 0.5% in the measuring range (0 up to 10 Bars). These measurements provide the average flow pressure at the pipe wall at each measurement cross-section.

2.1 Experimental results

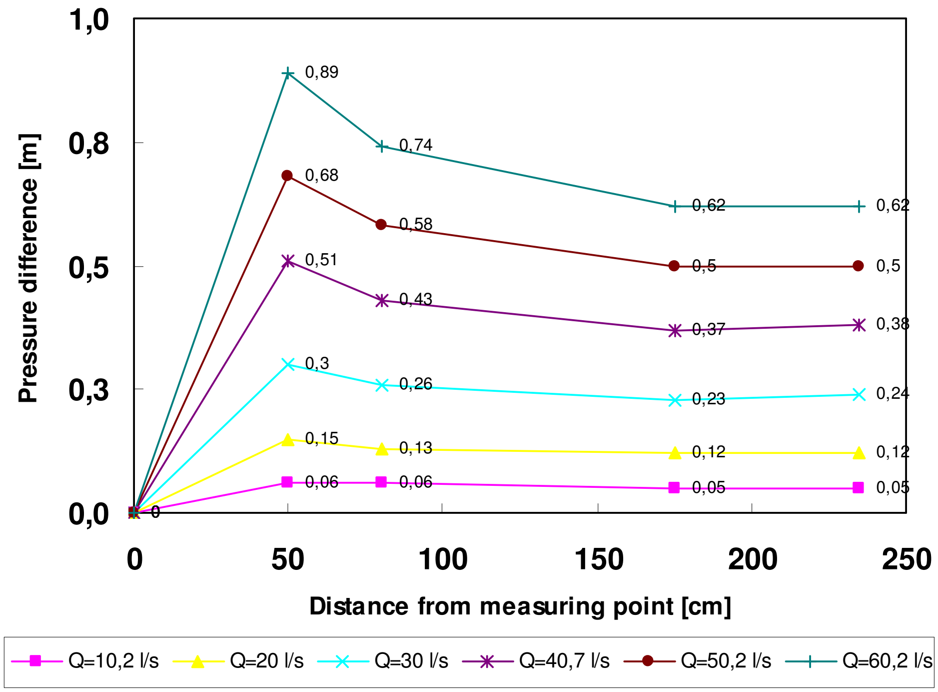

Figure 3 Pressure difference (relative to the pressure in front of the nozzle) as a function of the distance along the pipe in the “pump” flow direction for different flow rates.

The figure 3 clearly shows that the pressure drop produced by the nozzle, increases with higher capacity, according to transport and Bernoulli equations. When the distance from the nozzle (in direction that is opposite to flow direction) increase the pressure drop is decreased up to the final constant values. This flow pressure drop corresponds to the pressure loss at different – individual operating capacities.

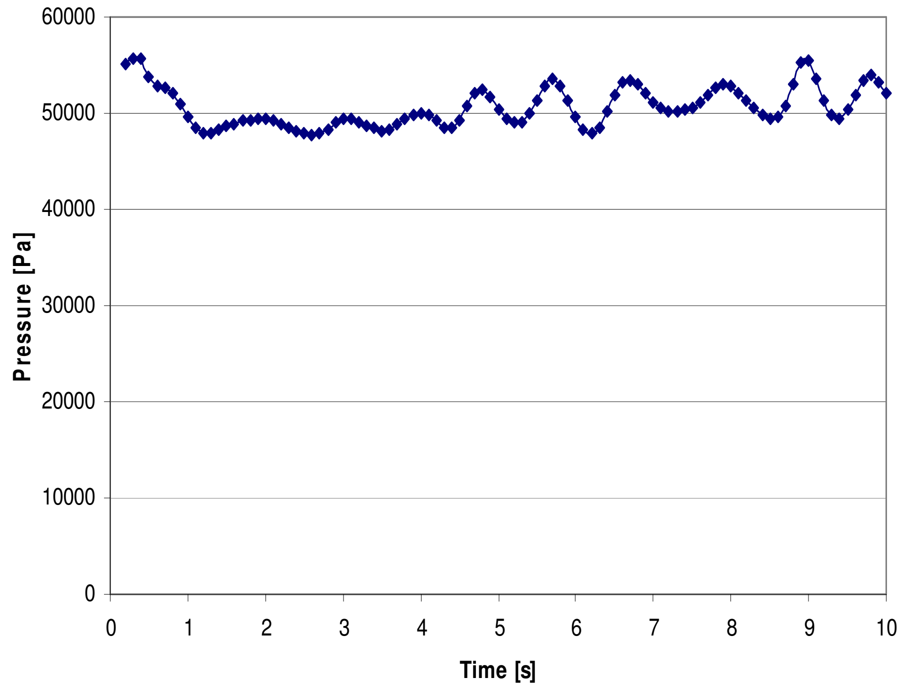

Figure 4 Time dependent flow pressure at measuring sector D-D in “turbine” flow direction.

The measurement at cross-section D-D shows an oscillating pressure as shown in the figure 4. These oscillations are interesting because no physical explanation is found. To explain these flow pulsations the numerical analysis were preformed.

3. NUMERICAL ANALYZE

3.1 Governing equations

3.1.1 The Continuity equation

Continuity equation is equation of the principle that mass is conserved. In differential form it can be written as

$$\frac{\partial \rho}{\partial t}+\frac{\partial u_j \rho}{\partial x_j}=0. \tag{1}$$

3.1.2 The Momentum equation

The momentum equation is basic equation of the Newton’s second law. In differential form it can be written as

$$\rho \frac{\partial u_i}{\partial t}+\rho u_j \frac{\partial u_i}{\partial x_j}=\rho f_{mi}+\frac{\partial \sigma_{ij}}{\partial x_j} \tag{2}$$

3.1.3 Turbulence models

The Reynolds averaged equations (RANS) with applying the Boussinesque approximation, assuming proportionality between the deviatory parts of the Reynold`s stress tensor and the strain rate tensor.

The standard k – ε turbulence model
For this model the transport equation for the turbulent kinetic energy *k* takes the form

$$\frac{\partial k}{\partial t}+\overline{u}_i\frac{\partial k}{\partial x_i}=\frac{\partial}{\partial x_i}\left[\left(\upsilon_0+\frac{\upsilon_T}{\sigma_k}\right)\frac{\partial k}{\partial x_i}\right]+P-\varepsilon\,, \tag{3}$$

where C_μ, σ_k, σ_ε, $C_{1\varepsilon}$ and $C_{2\varepsilon}$ present the model constants.

3.2 Numerical mesh and slower parameters

The calculation domain is a three dimensional volume, in our case, this volume was mashed with tetrahedron elements, (Figure 5) forming an unstructured mesh generated by CFX-Mesh. The mesh consists of 301565 elements with mesh refinement in the area of cross section change (as shown in Figure 6). The high velocity gradients in the boundary layer are captured using layers of prisms (for a total of 92919 prisms).

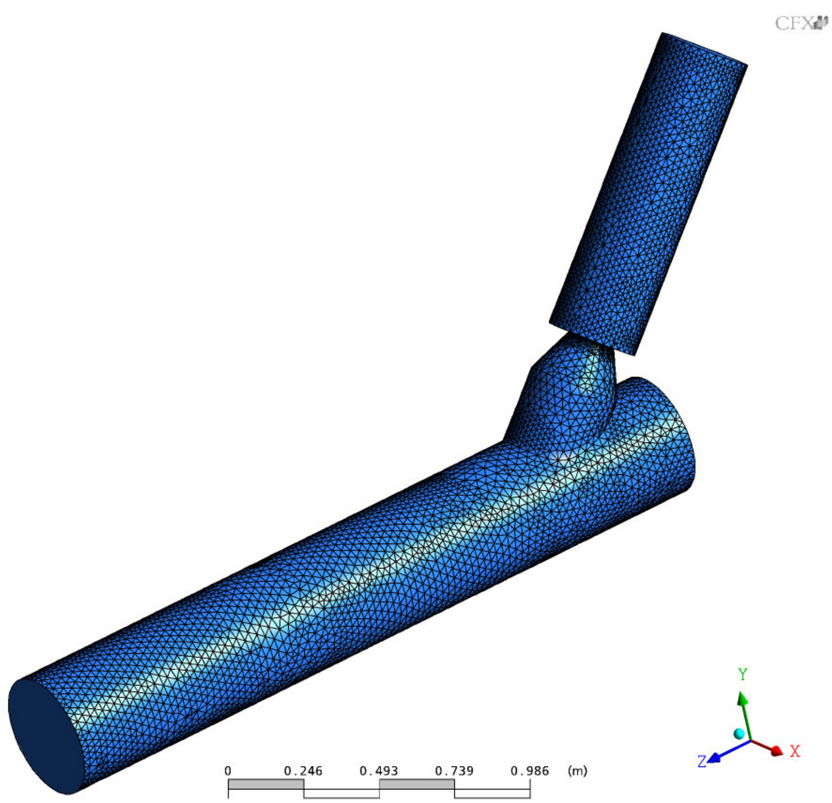

Figure 5 Numerical mesh of the pipe and nozzle at the junction.

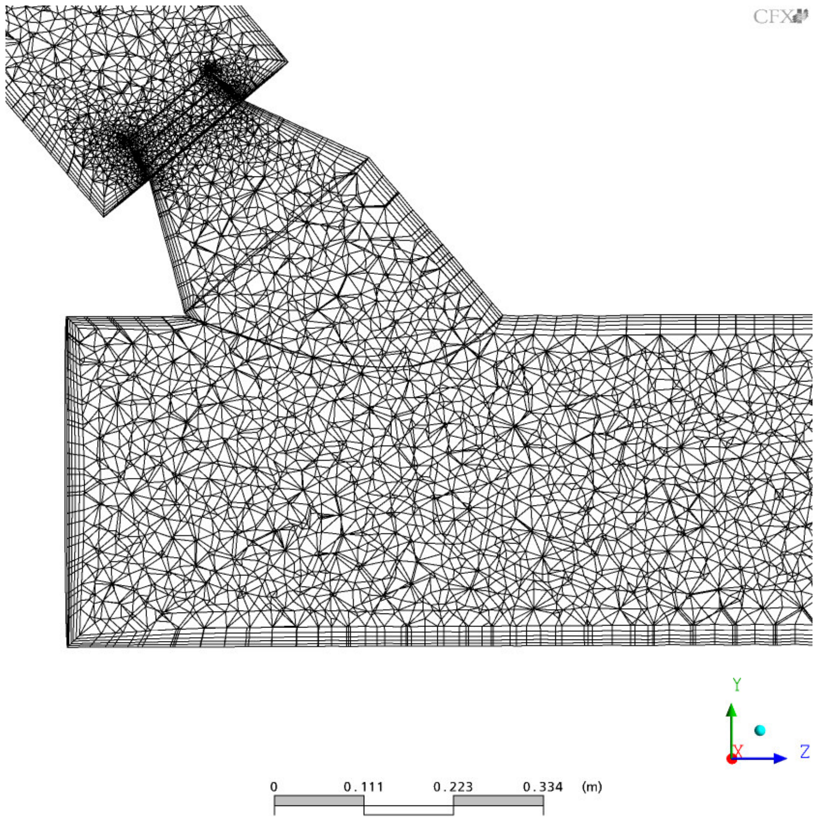

Figure 6 Detailed numerical mesh of nozzle.

3.2.1 Boundary conditions

Boundary conditions define the flow conditions across the boundary surfaces.

The following boundary conditions were defined in our case:

- the zero slip wall condition (the walls of the nozzle),
- inlet condition (the nozzle inlet),
- opening condition (the nozzle outlet).

The relative static pressure p = 120000Pa was prescribed at the inlet. The mass flow rate Q =110kg/s was prescribed at the outlet. The reference pressure was set to p_{atm}=101325Pa.

3.2.2 Solver parameters and convergence criteria

The residual target for all simulations was set to $r_{RMS}=10^{-4}$. From residual analysis, it was evident that the area where the residual target was not reached, the steady case of simulation is occurred. In the case of transient run, we defined 100 timesteps with 0.1 s increments and with a maximum number of 25 iterations (coefficient loops) per timestep.

3.3 Numerical results

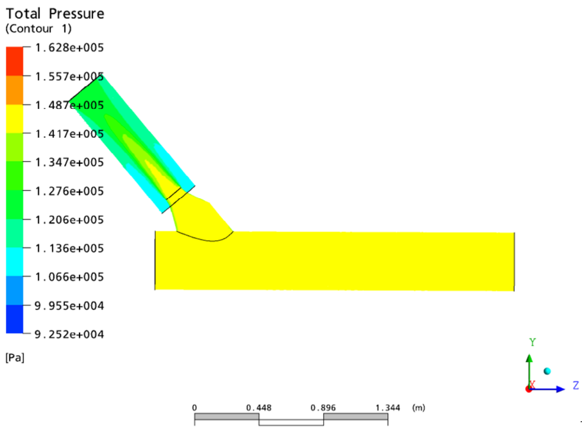

a)

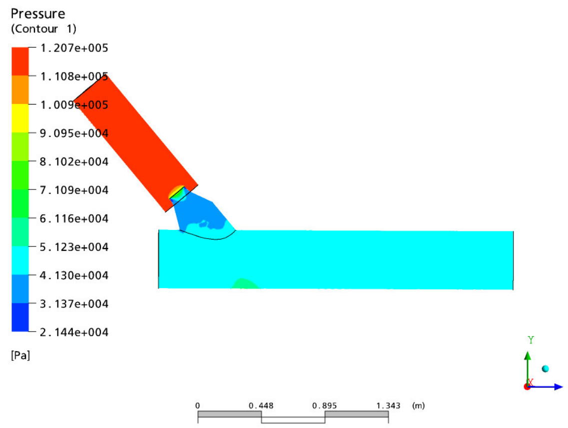

b)

Figure 7 Flow pressure in (a) “pump” and (b) in “turbine” operating regime.

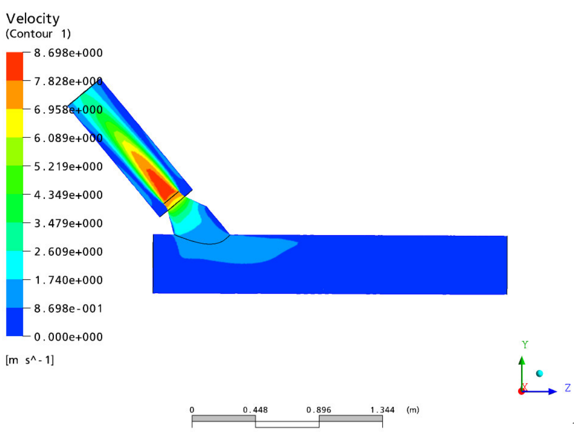

a)

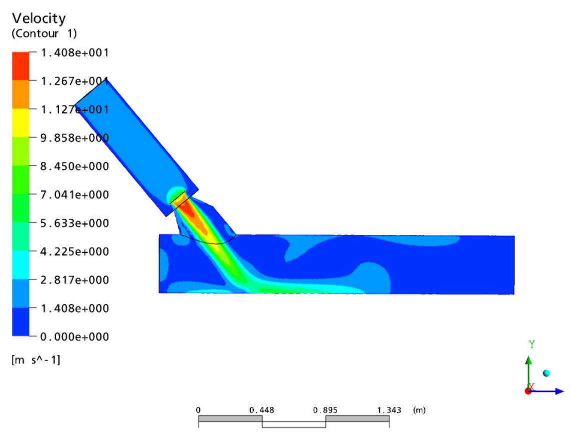

b)

Figure 8 Flow velocities in (a) “pump” and (b) in “turbine” operating regime.

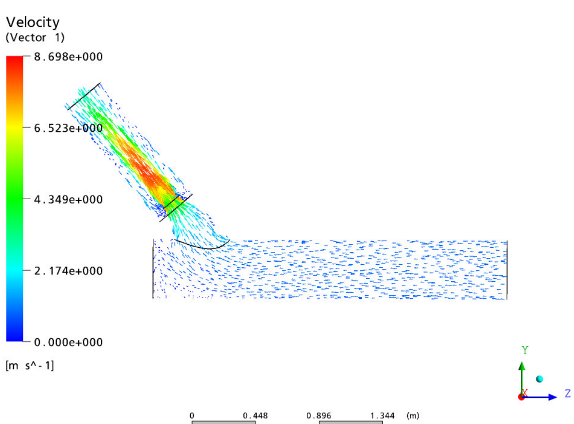

a)

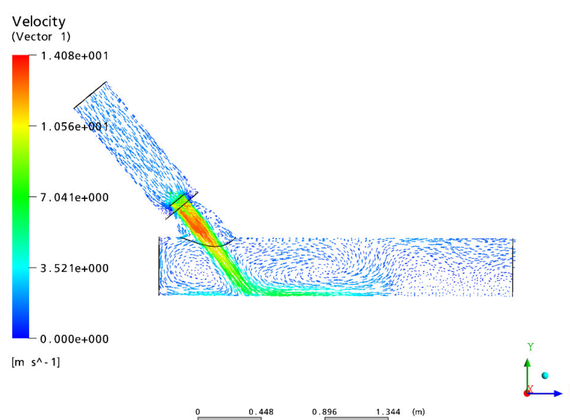

b)

Figure 9 Flow velocity vectors in (a) “pump” and (b) in “turbine” flow operating regime.

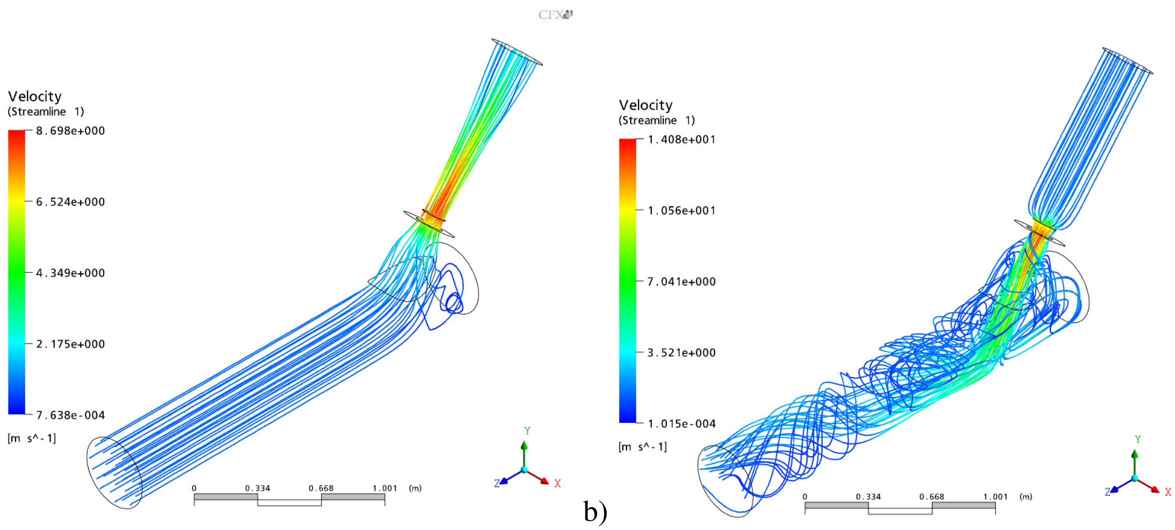

a) b)

Figure 10 Flow velocity streamlines in (a) "pump" and (b) in "turbine" flow direction.

From the numerical results of the pressure distribution through the nozzle for the "pump" operating regime, the pressure jet is evident (Figure 7.a). The jet is symmetrical with respect to the pipe axis. In the "turbine" operating regime the jet (Figure 7.b) is not clearly defined. This might be due to the nozzle geometry, since the nozzle cross-section in this direction gradually increases up to the pipe diameter in the flow direction for the "turbine" regime. The flow jets appear clearly in the flow velocity contour plots for both operating regimes (Figure 8). In the "turbine" operating regime the flow jet hits the pipe wall (Figure 8.b) where the material erosion is expected. The pipe wall loads could be determined from the numerical results. Using the velocity vector plots (Figure 9) the recirculating flow can be observed in the "turbine" operating regime (Figure 9.b). Two recirculation regions are well captured: one at the left side (back pipe position) and the other one in the right side, because of the flow jet in direction of the discharging pipe. This recirculating flow appeared at all calculated flow rates and it is a permanent phenomena. The recirculating flow is observed more clearly in the streamlines plots (Figure 10). Recirculating flow appears in the "pump" operating regime at back position (Figure 10.a). In the "turbine" operating regime is recirculating flow evident at both sides of the flow jet (Figure 10.b). In the discharge pipe right from the flow jet, the flow disorder is clearly present. We believe that the reason is in the 3D recirculation flow nature.

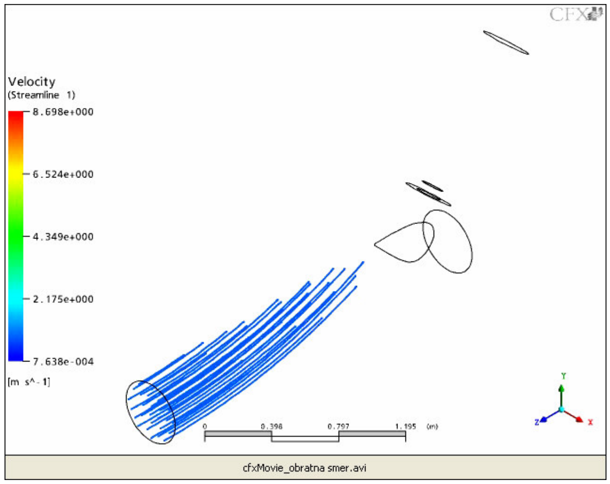

Figure 11 Simulation clip with velocity streamlines in “pump” flow direction.

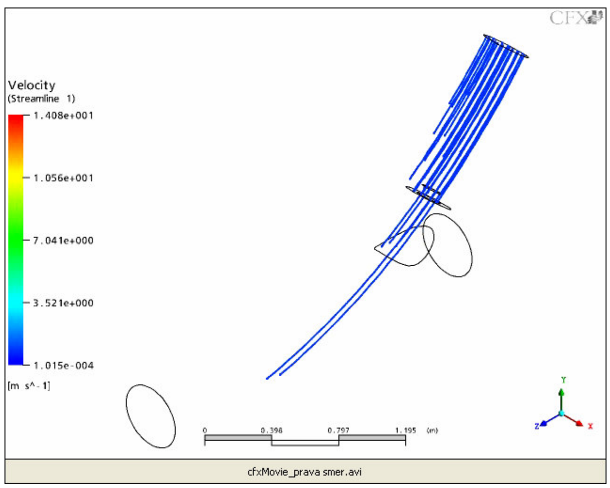

Figure 12 Simulation clip with velocity streamlines in “turbine” flow direction.

The recirculation flows are shown at the transient simulation animations at Figure 11 and 12.

4. CONCLUSIONS

Experimental and numerical analyses shows that there is essential to perform the physical model test for a numerical and experimental results confirmation.

The pressure measurement shows the pressure losses and their variations in the vicinity of the nozzle.

Performing the transient numerical calculations the dynamic loads on the pipe walls can be determined and the pipe can be properly dimensioned. Based on the presented analysis, similar simulations should be performed to increase the certainty, and we plane to perform more analyses on similar pipe systems.

REFERENCES

Bergant A. (2003). "The behavior of a hydraulic turbomachines during transients", Journal of Mechanical Engineering, Year 49, Vol. 3, pp 150-160.

Brennen, C. E. (1995). Cavitation and Bubble Dynamics. Oxford University Press, London.

Dular, M., Širok, B., Stoffel B., Bachert, B. (2003). "Numerical simulation of cavitation on a single hydrofoil in a cavitation tunnel", Slovene Society for Mechanics, 2003, Slovenia, pp 93-103.

Resiga, R., S., Muntean, S., Bernad, S., Anton, S. (2003), "Numerical investigation of 3D cavitating flow in Francis turbines", Proceedings of the Conference on Modeling Fluid Flow, Vol. 2, pp 950-957

White F. M. (1999). Fluid Mechanics, Forth Edition, McGraw-Hill International Editions.

ACKNOWLEDGEMENTS

Authors would like to thank to the staff of the Institute for water resources and management at Technology University of Graz, where experimental work were preformed.